Process Biochemistry 45 (2010) 549–555

Contents lists available at ScienceDirect

Process Biochemistry

journal homepage: www.elsevier.com/locate/procbio

Analysis of the rate-limiting step of an anaerobic biotrickling filter removing TCE vapors

Sudeep C. Popat [a], Marc A. Deshusses [b,*]

[a] Department of Chemical & Environmental Engineering, University of California, Riverside, CA 92521, United States
[b] Department of Civil & Environmental Engineering, Duke University, Durham, NC 27708, United States

ARTICLE INFO

Article history:
Received 26 June 2009
Received in revised form 19 November 2009
Accepted 28 November 2009

Keywords:
Biotrickling filter
Biofilter
TCE
Mass transfer
Biodegradation

ABSTRACT

A detailed analysis of a biotrickling filter treating trichloroethene (TCE) vapors anaerobically is presented and discussed. The biotrickling filter relies on mixed cultures containing bacteria from the genus *Dehalococcoides* that reductively dechlorinate TCE to ethene. After about 200 days of steady operation, as biomass in the packed bed increased, a partial loss in treatment performance was observed which prompted the present investigations. Analysis of TCE and of its degradation metabolites in the gas phase and in the trickling liquid combined with the calculation of global effectiveness factors revealed that significant mass transfer limitations existed. Depending on the conditions, either the gas film or the liquid film limited the removal of TCE. These findings were confirmed by the determination of gas and liquid films mass transfer coefficients. In all cases, removal of TCE was greater without trickling of liquid. The most plausible reason for the onset of mass transfer limitations was the decrease in the specific interfacial area brought by important biomass growth over time. Overall, this study illustrates how complex kinetic and transport limitations can vary with the operating conditions in biotrickling filters.

1. Introduction

Biological treatment of waste gases is rapidly gaining acceptance as a green alternative to conventional methods such incineration, adsorption onto activated carbon, and catalytic oxidation [1,2]. In particular, the development of biotrickling filters has resulted in greater volumetric throughput compared to traditional biofilters [3–5]. The principle of biotrickling filters is simple. Pollutant-degrading microorganisms are attached to an inert packing material or support and convert pollutants to benign products. An aqueous phase is continuously or intermittently trickled over the packed bed, providing essential nutrients to the microorganisms, leaching potential by-products and maintaining favorable conditions for the process culture.

Although simple in concept, the elimination of gaseous pollutants in biotrickling filters involves a series of complex physico-chemical and biological phenomena [6]. These are gas–liquid followed by liquid–biofilm or direct gas–biofilm mass transfer of the pollutant, pollutant diffusion within the biofilm and pollutant biodegradation in the biofilm. The majority of the pollutant is degraded by attached bacteria rather than by bacteria suspended in the trickling liquid [7]. Despite a growing body of research on biotrickling filters, the understanding of these phenomena and of their relevance to the overall treatment performance remains sketchy. As a result, biotrickling filters are frequently operated without knowledge of the rate-limiting step(s), and thus the true upper limits of attainable performance are not known.

For example, reports on H_2S removal in biological reactors show a vast range of elimination capacities for inlet concentrations in the range of 20–100 ppm_v [4,8–10]. It was not until Kim and Deshusses [11] studied the effect of gas velocity in detail using a differential biotrickling filter that it was understood that external mass transfer plays an important role in the removal of H_2S in biotrickling filters. This paved the way for the development of high performance biotrickling filters that are operated at extremely short gas residence times [4,5,12,13]. The question of the rate-limiting step was elegantly discussed by Lobo et al. [14] who defined the global effectiveness factor (η_0). This factor can easily be calculated from measured bulk gas and liquid concentrations of the pollutant. It represents the fraction of total resistance to pollutant removal due to biofilm phenomena (Table S1, see Supporting Information) while $1 - \eta_0$ is the fraction of the total resistance attributed to gas–liquid mass transfer. By combining the effectiveness factor with a detailed modeling of the biotrickling filtration process, and a model sensitivity analysis, Lobo et al. [14] illustrated how external transport and internal limitations changed along the height of the biotrickling filter and how co- and counter-current operations led to different reactor performance depending on the rate-limiting step.

* Corresponding author. Tel.: +1 919 660 5480; fax: +1 919 660 5219.
E-mail address: marc.deshusses@duke.edu (M.A. Deshusses).

1359-5113/$ – see front matter © 2009 Elsevier Ltd. All rights reserved.
doi:10.1016/j.procbio.2009.11.017

The challenge is then to use such information either for troubleshooting or for process optimization. In this paper, we present a detailed analysis of a biotrickling filter that experienced a loss in treatment performance. The biotrickling filter that was investigated was a novel anaerobic system treating trichloroethene (TCE) vapors using microorganisms from the genus *Dehalococcoides*. When provided with a suitable electron donor, these microorganisms reductively dechlorinate TCE through cis-dichloroethene (cis-DCE) and vinyl chloride (VC) to ethene, by progressive dehalogenation in a series of two electrons reductions (TCE → cis-DCE → VC → ethene). Microorganisms from the genus *Dehalococcoides* are increasingly being used for *in situ* bioremediation of chlorinated solvents through bioaugmentation [15]. We deployed *Dehalococcoides* sp. in a laboratory-scale biotrickling filter and demonstrated that TCE vapors in nitrogen gas could be effectively eliminated [16]. Lactate served as substrate for fermenting organisms producing hydrogen which was used as electron donor for TCE dehalogenation by *Dehalococcoides* sp.

After about 220 days of continuous operation, the TCE elimination capacity (EC) dropped from about 2.9 to 1.3 g m_{bed}^{-3} h^{-1}. This coincided with the visual observation that an important amount of biomass had accumulated in the packed bed, which was confirmed by gravimetric analysis. Thus plugging of the bed occurred, despite the fact that the organic loading was relatively low compared to biotrickling filters treating volatile organic compounds and that growth yields for anaerobic microorganisms are at least an order of magnitude lower than those for aerobic microorganisms [17]. These observations triggered the experiments reported in this paper, aimed at the determination of the rate-limiting step(s) for TCE treatment in the biotrickling filter after the performance had dropped. This was accomplished by quantifying the global effectiveness factor and a greater understanding of TCE mass transfer was obtained by determining gas and liquid films mass transfer coefficients. The systematic and comprehensive study of the rate-limiting step provided a detailed insight into the fundamental mechanisms of pollutant removal in biotrickling filters.

2. Materials and methods

2.1. Biotrickling filter setup

The biotrickling filter setup was the same as described by Popat and Deshusses [16] (see Fig. S2, see Supporting Information). A biotrickling filter configuration was selected as the recirculating liquid provides an easy means to supply lactate and control the pH, which would not be possible in a biofilter system. Briefly, the biotrickling filter was constructed from a clear PVC pipe 60 cm in height and 10 cm in internal diameter (Harrington Plastics, Riverside, CA). It was packed with cattle bone porcelite (CBP), a porous spherical packing material with slow-release nutrients incorporated (Aisin Takaoka Co., Ltd., Japan). The spherical beads had an average diameter of 3 mm, and the specific surface area was determined to be 1160 m^2 m_{bed}^{-3} as per Ottengraf [18]. The active bed height was 30 cm, and thus the bed volume 2.4 L. The initial bed porosity was 0.42. The bed was inoculated with SDC-9™, a commercially available mixed bacterial culture (Shaw Environmental Inc., Lawrenceville, NJ) that contains at least two *Dehalococcoides* sp., fermenters that produce hydrogen, and methanogens (personal communication from Robert J. Steffan, Shaw Environmental Inc., Lawrenceville, NJ).

TCE (dimensionless Henry's constant 0.392 at 25 °C) vapors in humidified nitrogen gas (180–210 mg_{TCE} m^{-3}) was fed to the biotrickling filter from the top, resulting in downflow co-current operation mode. A nutrient solution was continuously recirculated over the bed from the sump (300 mL in this study) at the bottom of the biotrickling filter. Fresh nutrient solution (modified RAM media, Table S2, see Supporting Information) supplemented with 2.1–2.5 g L^{-1} sodium lactate (60%, w/w sodium lactate solution, Fisher Chemical, Fairlawn, NJ) was continuously added to the sump at the flow rate of 0.55 mL min^{-1}. This lactate feeding rate corresponds to 10 times the stoichiometric requirement for producing hydrogen necessary for complete TCE dechlorination. Periodic total organic carbon analyses of the recycle liquid confirmed that lactate was provided in excess as not all lactate fed was consumed.

2.2. Effect of liquid and gas velocities

All experiments on the effect of liquid (0.09–0.59 m h^{-1}) and gas (2.68–6.11 m h^{-1}) velocities were done from day 270 after the initial startup onwards. These experiments involved determination of the TCE elimination capacity (EC, see Eq. (1)), as well as the global effectiveness factor [14] (η_0, see Eq. (2)) for TCE, cis-DCE, VC and ethene at the bottom of the biotrickling filter. The latter required measuring the concentration of each compound not only in the outlet waste gas stream but also the liquid sump.

$$EC = \frac{Q_G(C_{G,in} - C_{G,out})}{V_b} \quad (1)$$

$$\eta_0 = \frac{HC_L}{C_G} \quad (2)$$

All reported values of the TCE EC and the global effectiveness factors are from an average of analysis from at least three gas and liquid samples. After a change in condition, the biotrickling filter was allowed to reach pseudo steady state before analysis, which was achieved in 1.5–2 h.

2.3. Determination of liquid film and gas film mass transfer coefficients

For the determination of the liquid film mass transfer coefficient (k_La_W in which the w stands for the wetted area) at different liquid velocities, absorption of hexane vapors into trickling water was used. Hexane was not biodegraded by the culture in the biotrickling filter. It is hydrophobic and only slightly soluble in water (dimensionless Henry's constant = 74; water solubility = 13 mg L^{-1} at 25 °C) and thus most of the resistance to its gas–liquid mass transfer is in the liquid film. The influent waste gas stream was laden with hexane vapors (600–800 mg m^{-3}) instead of TCE. The nutrient solution was replaced with water, which was trickled through the bed (one-pass) at different liquid velocities (0.09–0.59 m h^{-1}). A fixed gas velocity of 4.59 m h^{-1} was used. The steady state concentrations of hexane in the gas and liquid outlet streams were used to calculate the liquid film mass transfer coefficient from Eq. (3).

$$k_La_W = \frac{Q_L}{V_b}\ln\left(\frac{C_G/H}{C_G/H - C_{L,out}}\right) \quad (3)$$

For the determination of the gas film mass transfer coefficient (k_Ga_W) at different gas velocities (2.68–6.11 m h^{-1}), absorption of methyl *tert*-butyl ether (MTBE) vapors into water was used. MTBE was not biodegraded by the culture in the biotrickling filter. It is highly soluble in water (dimensionless Henry's constant = 0.023; water solubility = 50 g L^{-1} at 25 °C), and thus most of the resistance to its gas–liquid mass transfer is in the gas film. The influent waste gas stream was laden with MTBE vapors (200–300 mg m^{-3}) instead of TCE, and water was trickled through the bed (one-pass) at a fixed velocity of 0.27 m h^{-1}. The steady state concentrations of MTBE in the inlet and outlet gas streams were used to calculate the gas film mass transfer coefficient from Eq. (4).

$$k_Ga_W = \frac{Q_G}{V_b}\ln\left(\frac{C_{G,in}}{C_{G,out}}\right) \quad (4)$$

2.4. Analytical techniques

Gas phase concentrations of TCE, cis-DCE, VC, ethene, methane, hexane and MTBE were quantified using an HP 5890 Series II gas chromatograph, fitted with a 30 m (0.32 mm internal diameter) GS-Q column (Agilent Technologies Inc., Wilmington, DE) and a flame ionization detector. 5 mL of gas was injected per sample using a gas injection loop. The liquid concentrations of each compound were quantified by placing at least 10 mL of liquid sample in sealed vials of at least 40 mL allowing the compounds to reach gas–liquid equilibrium for at least 1 h, and then analyzing the gas headspace as described above. The liquid concentrations were calculated from the gas concentrations using the temperature-dependent Henry's constant for each compound [19–21]. This method was validated by using known concentrations of target compounds in deionized water, analyzing the gas headspace after equilibrium and confirming the initial liquid concentrations calculated from the analyzed gas concentrations. The dynamic liquid hold-up of the bed was determined by stopping the liquid recirculation at each liquid velocity, and then collecting the liquid draining for 30 min. Pressure drop across the biotrickling filter bed was measured using a U-tube manometer.

3. Results

3.1. Effect of liquid velocity

The effect of the liquid trickling velocity on the TCE EC and on the global effectiveness factor of TCE ($\eta_{0,TCE}$) is shown in Fig. 1a and b, respectively. The TCE EC of the biotrickling filter increased from 1.33 to 1.70 g m_{bed}^{-3} h^{-1} as the liquid velocity was increased from 0.09 m h^{-1} to 0.27 m h^{-1}. Subsequent increases in liquid velocity, however, did not improve the TCE EC. Interestingly, the TCE EC was

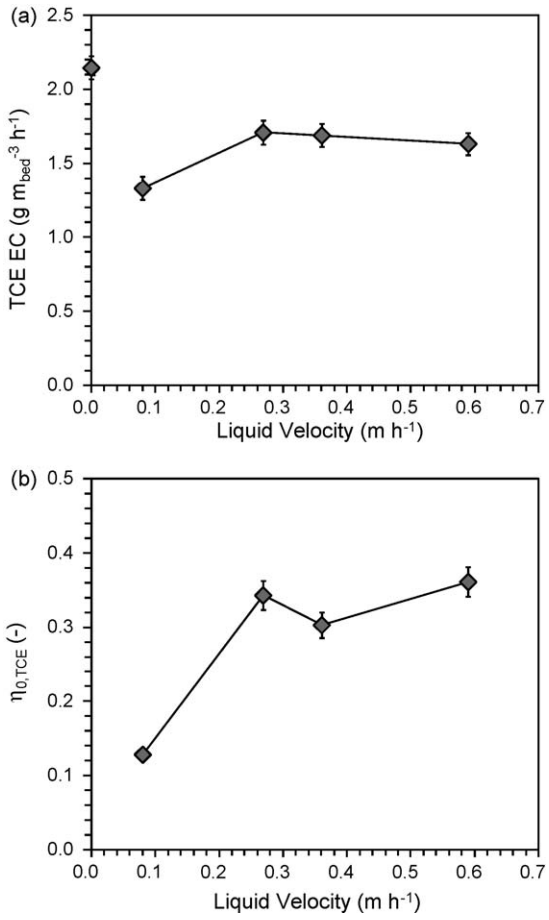

Fig. 1. Effect of liquid velocity on (a) TCE elimination capacity (EC) and (b) $\eta_{0,TCE}$ at a constant gas velocity of 4.59 m h^{-1}. The error bars show uncertainties in calculated values on the basis of standard deviations in each concentration from at least three analytical samples.

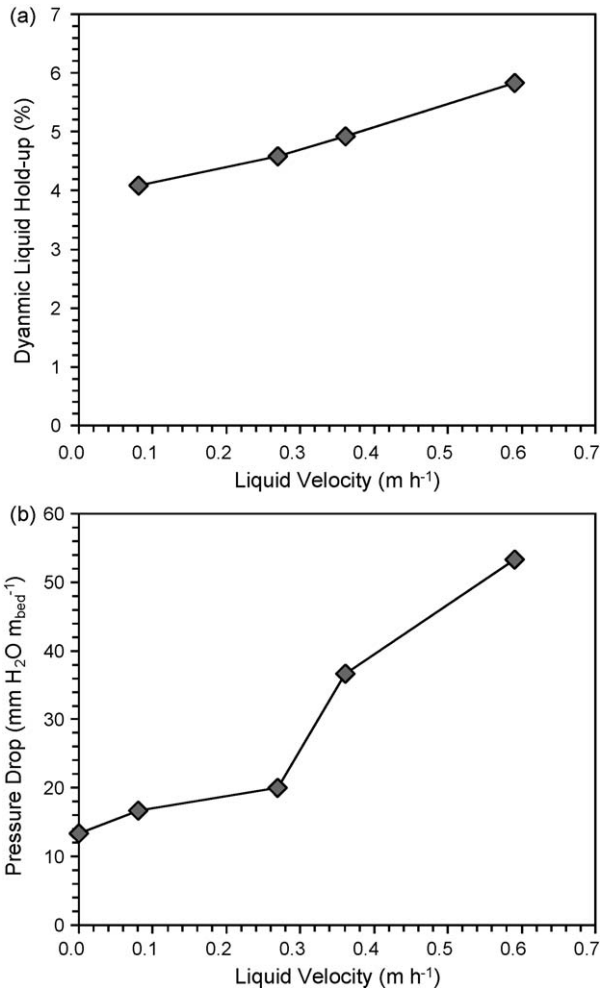

Fig. 2. Effect of liquid velocity on (a) dynamic liquid hold-up and (b) pressure drop at a constant gas velocity of 4.59 m h^{-1}. The uncertainty in the analysis of dynamic liquid hold-up was 5% while that in the analysis of pressure drop was 10%.

the highest (2.14 g m$_{bed}^{-3}$ h^{-1}) without any liquid trickling, stimulating the investigations reported in this paper. $\eta_{0,TCE}$ increased from 0.13 to 0.34 with an increase in liquid velocity from 0.09 m h^{-1} to 0.27 m h^{-1}, but did not change significantly with further increase in liquid velocity. $\eta_{0,cis\text{-}DCE}$, $\eta_{0,VC}$ and $\eta_{0,ETH}$ at different liquid velocities are shown in Table S3 (see Supporting Information). Briefly, all values of $\eta_{0,cis\text{-}DCE}$, $\eta_{0,VC}$ and $\eta_{0,ETH}$ were greater than 1 (as can be expected from by-products of biodegradation) and followed the trend $\eta_{0,cis\text{-}DCE} < \eta_{0,VC} < \eta_{0,ETH}$.

The dynamic liquid hold-up of the biotrickling filter and the pressure drop across the bed at different liquid velocities are shown in Fig. 2a and b, respectively. Both the dynamic liquid hold-up and the pressure drop across the bed increased over the range of liquid velocities that were tested. The relative increase in the pressure drop was much greater than the increase in dynamic hold-up.

3.2. Effect of gas velocity

The effect of gas velocity on the TCE EC and on the effectiveness factor of TCE is shown in Fig. 3a and b, respectively. A liquid velocity of 0.27 m h^{-1} was chosen for these experiments, since the results of Fig. 2b show a large pressure drop at higher liquid velocities. The gas velocities were changed from 2.68 m h^{-1} to 6.11 m h^{-1}, resulting in EBRTs of 3 min to 6.8 min. The TCE EC increased linearly from 1.13 g m$_{bed}^{-3}$ h^{-1} to 1.84 g m$_{bed}^{-3}$ h^{-1}, with increasing gas velocity. Similarly, $\eta_{0,TCE}$ increased linearly, reaching 0.44 at the highest gas velocity. $\eta_{0,cis\text{-}DCE}$, $\eta_{0,VC}$ and $\eta_{0,ETH}$ at different gas velocities are shown in Table S4 (see Supporting Information). Briefly, all values of $\eta_{0,cis\text{-}DCE}$, $\eta_{0,VC}$ and $\eta_{0,ETH}$ were greater than 1 and followed the trend $\eta_{0,cis\text{-}DCE} < \eta_{0,VC} < \eta_{0,ETH}$.

3.3. Effect of gas velocity without trickling liquid

The effect of gas velocity on the TCE EC without any liquid trickling is shown in Fig. 4. Since the trickling liquid was the medium to deliver lactate, the hydrogen source, to the bed, it was first necessary to evaluate how long TCE removal performance was maintained in the absence of the liquid. It was found that the reactor was able to sustain a steady removal of TCE for 4–6 h after stopping the trickling liquid (data not shown), after which the performance started to decrease. Thus, all TCE ECs determined for the different gas velocities are from gas analyses done between 1.5 and 3 h after stopping the liquid trickling. The TCE EC increased from 1.51 g m$_{bed}^{-3}$ h^{-1} to 2.09 g m$_{bed}^{-3}$ h^{-1} with increases in gas velocity from 2.68 m h^{-1} to 6.11 m h^{-1}. There was however no significant change between the increase in gas velocity from 4.59 m h^{-1} to 6.11 m h^{-1}. At all gas velocities, the TCE elimination capacity was higher without trickling liquid than with liquid velocity of 0.27 m h^{-1} (compare Figs. 3a and 4).

4. Discussion

As mentioned in the introduction, Lobo et al. [14] defined the global effectiveness factor (η_0, see Eq. (2)), which quantifies the

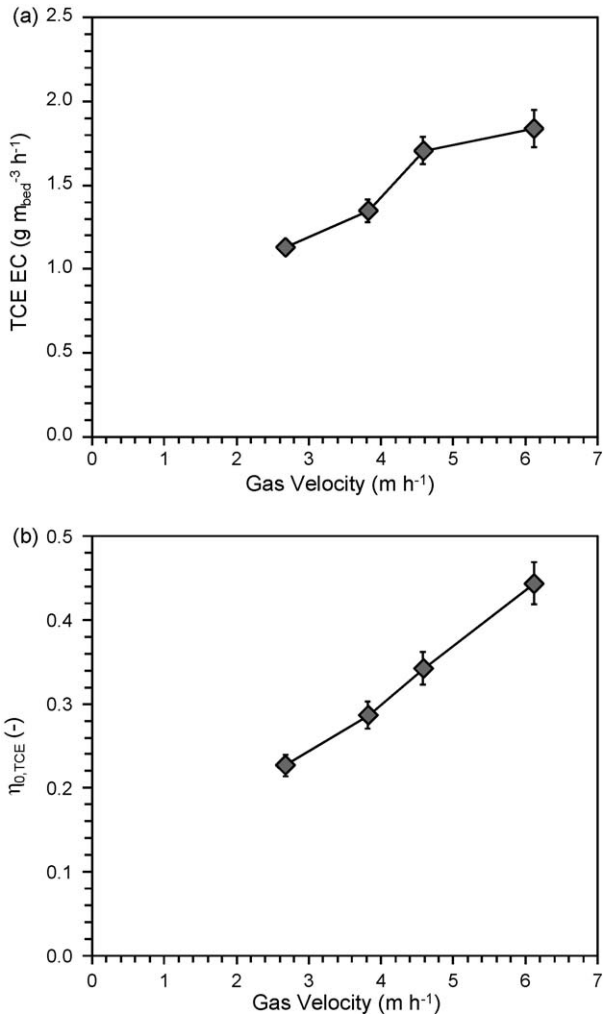

Fig. 3. Effect of gas velocity on (a) TCE elimination capacity (EC) and (b) $\eta_{0,TCE}$ at a constant liquid velocity of 0.27 m h^{-1}. The error bars show uncertainties in calculated values on the basis of standard deviations in each concentration from at least three analytical samples.

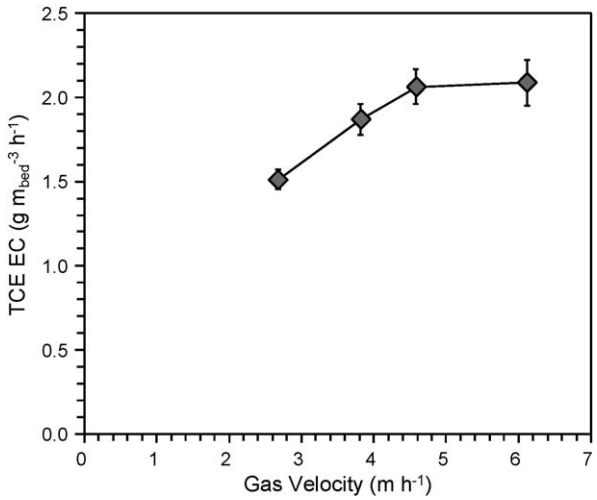

Fig. 4. Effect of gas velocity on TCE elimination capacity (EC), with no trickling liquid. The error bars show uncertainties in calculated values on the basis of standard deviations in each concentration from at least three analytical samples.

fraction of the total resistance to removal of a pollutant from biofilm phenomena (Table S1, see Supporting Information). Within biofilm phenomena, however, η_0 does not allow distinguishing between liquid–biofilm mass transfer limitation, diffusion in the biofilm and biodegradation limitation. Similarly, $1 - \eta_0$ is the fraction of resistance attributed to gas–liquid mass transfer.

The global effectiveness factor can be calculated from gas and liquid concentrations of the pollutant of interest throughout the entire height of the bed. The value of the global effectiveness factor for co-current operation of biotrickling filters starts at 0 at the top of the column, and can increase along the axial direction to reach a maximum value of 1. A value of 0.5 means equal resistance from biofilm phenomena and gas–liquid mass transfer, and thus for values less than 0.5 the process can be said to be gas–liquid mass transfer limited and for values greater than 0.5 biofilm phenomena limited. As will be emphasized later, these quantitative considerations on η_0 are only valid for the pollutant undergoing treatment. For metabolites produced in the biofilm, the reasoning should be reversed and η_0 values greater than 1 indicate some gas–liquid mass transfer limitation. For a given specific surface area and pollutant biodegradation rate, whether or not and how fast η_0 reaches 1 depends on the gas–liquid transfer properties of the pollutant. For example, Fortin and Deshusses [22] determined the global effectiveness factor values for MTBE at the top and bottom of the bed in a biotrickling filter, and found that by the time the gas reached the bottom of the bed, gas–liquid equilibrium was reached, suggesting biofilm phenomena limited performance. Cox et al. [23] reported that global effectiveness factor for ethanol in a thermophilic biotrickling filter reached 1 within the first 20% of the 1 m long column; again suggesting biofilm phenomena limited performance. For both cases, the Henry's constants of the pollutants were low (H_{MTBE} = 0.03; $H_{EtOH,53\ ^{\circ}C}$ = 0.0009), and thus it was expected that the mass transfer rates would be high.

The main objective of this study was to determine the rate-limiting step for TCE removal after the important biomass build-up in the biotrickling filter. This was accomplished by determining the TCE EC and $\eta_{0,TCE}$ at different operating conditions, and determining gas and liquid film mass transfer coefficients. Because of the relatively low void volume of the packed bed (porosity 42%), it was not possible to determine $\eta_{0,TCE}$ throughout the height of the bed and only values at the bottom of the reactor were determined. Also, one important assumption was that the biotrickling filter was not limited by hydrogen availability. This is reasonable, because: (i) a 10-fold excess lactate vs. stoichiometric hydrogen requirement for complete TCE dechlorination was provided, and (ii) hydrogen is produced in the biofilm, and thus is not subjected to gas–liquid mass transfer limitations. Hydrogen availability was confirmed by monitoring methane production by methanogens present in the process culture which revealed that it was unaffected by the gas/liquid perturbations (data not shown). Other competing processes for hydrogen consumption, such as sulfate reduction as shown by Aulenta et al. [24], were not expected since alternate electron acceptors were excluded from the mineral medium.

4.1. Effect of liquid velocity

First, the effect of recirculating liquid velocity was determined (Fig. 1a and b). At the lowest liquid velocity (0.09 m h^{-1}), $\eta_{0,TCE}$ was 0.13, indicating that significant gas–liquid mass transfer limitation existed. Gas–liquid mass transfer is often modeled using the two-film theory [25]. The model assumes that species being transferred are in equilibrium at the gas–liquid interface. If resistance in the liquid film limits mass transfer, increasing the liquid velocity increases the rate of mass transfer. This is because a higher liquid velocity results in greater convective transport. In our experiments, increasing the liquid velocity from 0.09 m h^{-1} to 0.27 m h^{-1} resulted in greater TCE EC and a higher $\eta_{0,TCE}$. This indicates that gas–liquid mass transfer at the liquid film limited the overall removal at the lowest liquid velocity. Further increases in liquid velocity resulted in

no significant change in $\eta_{0,TCE}$ or TCE EC. An explanation for this can be derived by looking at the pressure drop data (Fig. 2b), which shows important pressure drop increases for small increases in liquid velocity. This suggests that the bed permeability was affected, as expected for a reactor close to clogging, and that additional liquid was pooling in key gas channels rather than being evenly distributed over the packing. Examination of the dynamic hold-up data (Fig. 2a) reveals that the reactor was not experiencing traditional flooding during these experiments. This is only because gas and water flowed co-currently, resulting in bubbling regime rather than complete flooding [26]. Nonetheless, pollutant elimination can be a direct function of the liquid distribution [27], and thus under bubbling regime, channeling of liquid and thus irregular distribution, most likely affected the TCE EC.

If indeed gas–liquid mass transfer is rate-limiting during treatment of TCE, one would expect that the metabolites of TCE dechlorination will not reach gas–liquid equilibrium, but instead be present in excess in the liquid phase, resulting in a value of η_0 greater than 1. This was indeed the case: $\eta_{0,cis\text{-}DCE}$, $\eta_{0,VC}$ and $\eta_{0,ETH}$ were all >1 at most liquid velocities (see Table S3), suggesting that gas–liquid equilibrium for all three compounds was not reached. Only $\eta_{0,cis\text{-}DCE}$ reached 1 with increasing liquid velocity. This can be explained by the fact that cis-DCE is the compound with the lowest Henry's constant. cis-DCE has a Henry's constant of 0.167 at [21], while for VC and ethene it is 1.167 and 8.52, respectively [20,21] (all at 25 °C). Hence cis-DCE will be subjected to the lowest resistance to liquid–gas mass transfer, and thus have η_0 values closest to 1. Values of η_0 for VC and ethene were consistent with their Henry's constant ($H_{cDCE} < H_{VC} < H_{Ethene}$).

Further insight into the trend observed in the effect of liquid velocity on the TCE EC and $\eta_{0,TCE}$ is obtained by looking at liquid film mass transfer coefficients (k_La_W). At a constant gas velocity, k_La_W increased from 4.28 h^{-1} to 5.67 h^{-1} when the liquid velocity was increased from 0.09 m h^{-1} to 0.27 m h^{-1} (Fig. 5). Further increases in liquid velocity resulted only in negligible increases in k_La_W. This was expected if the bed was close clogging. Increasing the liquid velocity in this case results in preferential flow paths for the gas and the liquid, thus lowering the interfacial area for gas–liquid mass transfer.

The importance of the liquid film mass transfer limitation on the removal of TCE was illustrated by calculating the maximum TCE mass transfer rate assuming liquid film resistance to be governing gas–liquid mass transfer. This was done by using the overall mass transfer coefficient (K_La_W) values calculated from the k_La_W values as determined earlier and the k_Ga_W value as determined later. The rates of TCE mass transfer calculated correlated well with the observed TCE EC (Fig. S2, see Supporting Information). This reinforces the fact that liquid film mass transfer resistance was an important rate-limiting step, especially at the lowest and the higher liquid velocities.

4.2. Effect of gas velocity

The effect of gas velocity was determined at a constant liquid velocity to determine to what extent the gas side of mass transfer limited the removal. Both the TCE EC and $\eta_{0,TCE}$ increased linearly with increasing gas velocity (Fig. 3a and b). Consistent with this result, $\eta_{0,TCE}$ remained below 0.5 at all gas velocities, suggesting that gas–liquid mass transfer was rate-limiting, but at the highest gas velocity tested (6.11 m h^{-1}), $\eta_{0,TCE}$ approached 0.5. This indicates that as gas velocity increased to the upper end of the range tested, biofilm phenomena started to become partially limiting TCE removal. A possible alternative explanation to the higher TCE EC with increasing the gas velocity is that increasing gas velocity (at a constant inlet concentration) increases the average pollutant concentration in the system, which can increase the EC if biodegradation is the rate-limiting step. However, this was not the case here. At the current conditions, the TCE EC was not sensitive to the TCE inlet concentration (Fig. S3, see Supporting Information) indicating that biodegradation was not rate-limiting. Consequently, at the conditions tested, it was the gas–liquid mass transfer that limited TCE removal. As discussed below, this conclusion is supported by gas–liquid mass transfer coefficient determinations and by experiments in which TCE was provided via the liquid rather than via the gas phase. Similar to the experiments on the effect of liquid velocity, the global effectiveness factors for the TCE dechlorination metabolites were greater than 1, and followed the trend $\eta_{0,cis\text{-}DCE} < \eta_{0,VC} < \eta_{0,ETH}$, which, as mentioned earlier, is consistent with the respective values of Henry's constants.

Further insight into the trend observed for the effect of gas velocity on the process is gained by looking at gas film mass transfer coefficients (k_Ga_W) determined for different gas velocities (Fig. 6). k_Ga_W increased linearly from 9.14 h^{-1} to 17.23 h^{-1} with an increase in gas velocity from 2.68 m h^{-1} to 6.11 m h^{-1}. A special attention to the wetted area is warranted. For reactors with counter-current flow

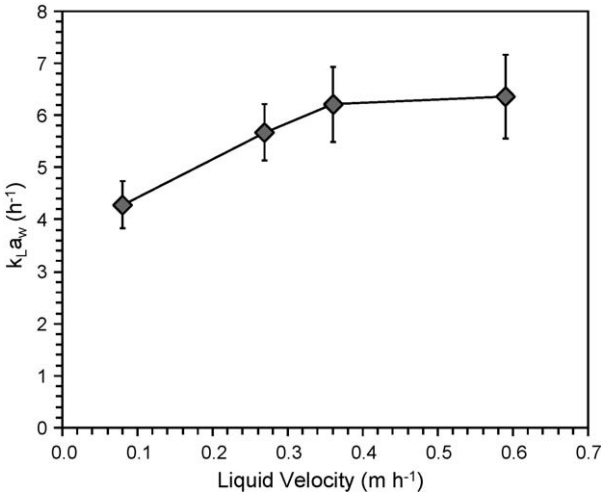

Fig. 5. Effect of liquid velocity on k_La_W at a constant gas velocity of 4.59 m h^{-1}. The error bars show uncertainties in calculated values on the basis of standard deviations in each concentration from at least three analytical samples. The uncertainties in the liquid velocity and the biotrickling filter bed volume were not considered.

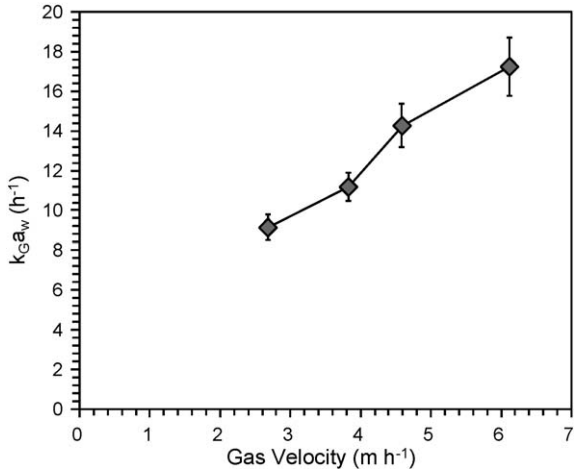

Fig. 6. Effect of gas velocity on k_Ga_W at a constant liquid velocity of 0.27 m h^{-1}. The error bars show uncertainties in calculated values on the basis of standard deviations in each concentration from at least three analytical samples. The uncertainties in the liquid velocity and the biotrickling filter bed volume were not considered.

operated at constant liquid velocities, the interfacial area available for gas–liquid mass transfer does not change significantly with different gas velocities [28]. However, for co-current operation, an increase in gas velocity can result in a lower liquid hold-up [29], and thus depending on the flow regime (trickling, pulsing or bubbling) gas velocity may affect the specific (wetted) surface area. On the other hand, increasing gas velocity results in a thinner gas film (higher k_G), which thus can improve the mass transfer rate.

The importance of the gas film mass transfer limitation in the removal of TCE was illustrated by calculating the maximum TCE mass transfer rate assuming gas film resistance to be governing gas–liquid mass transfer. This was done by using the overall mass transfer coefficient ($K_G a_W$) calculated from the $k_L a_W$ and the $k_G a_W$ values as determined earlier. The rates of TCE mass transfer calculated correlated well with the observed TCE EC (Fig. S4, see Supporting Information). This reinforces the fact that gas film mass transfer resistance was an important rate-limiting step when the bioreactor was operated at moderate liquid velocities.

Further confirmation of gas–liquid mass transfer limitation was provided by performing an experiment without any gas flow. TCE was supplied via the trickling liquid (liquid velocity 0.27 m h^{-1}) at a loading similar to an experiment that resulted in the TCE (vapor) elimination capacity of 1.7 g m_{bed}^{-3} h^{-1}. Under these conditions (i.e. direct TCE transfer from the liquid to the biofilm), the TCE EC was 1.94 g m_{bed}^{-3} h^{-1}, i.e. 14% higher than when TCE had to transfer from the gas to the liquid, and then to biofilm. A higher TCE EC for the direct liquid–biofilm mass transfer condition confirmed that under the conditions reported in this paper, reactor performance was limited by gas–liquid mass transfer.

4.3. Mass transfer limitation resulting from decrease in surface area

Before important biomass build-up in the reactor, the biotrickling filter had a TCE EC of 2.9 g m_{bed}^{-3} h^{-1}, and the performance was limited by biofilm phenomena ($\eta_{0,TCE}$ = 0.8–1.0, data not shown). The highest observed TCE EC at different gas and liquid velocities after the excess biomass build-up was 1.86 g m_{bed}^{-3} h^{-1}, and gas–liquid mass transfer limited the performance. One explanation for this difference is a marked decrease in the biofilm specific interfacial area because of biomass growth, thus shifting the rate-governing step from biofilm phenomena to gas–liquid mass transfer [30]. Alonso et al. [31] proposed a model for determining the specific interfacial area of beds packed with spherical packing on which biofilm grows. For spherical packing, the interfacial area depends on the biofilm thickness and the number of individual spheres in contact. Model and experiments showed that for any individual sphere, if four or more other spheres are in contact, an increase in biofilm thickness results in a decrease in surface area and bed porosity. Dullien [32] proposed a formula for determining the number of contact points for an individual sphere in beds packed with regular packing, on the basis of the bed porosity (see Eq. (5)). Using the initial bed porosity of 0.42 for the reactor bed in this study, the number of individual spheres in contact was determined to be 8, and thus biomass build-up is expected to result in a lower specific surface area.

$$\varepsilon = 1.072 - 0.1193n + 0.004312n^2 \quad (5)$$

4.4. Effect of gas velocity without trickling liquid

It is interesting to note that without any trickling liquid, the TCE EC (at all gas velocities) was higher than that at the liquid velocity of 0.27 m h^{-1} (compare Figs. 3b and 4). This is consistent with the above demonstration that either the gas or the liquid side of gas–liquid mass transfer was rate-limiting. Intermittent trickling has been shown by others to improve performance in some biotrickling filters, when limited by gas–liquid mass transfer [33,34]. At the highest gas velocities tested (4.59 m h^{-1} and 6.11 m h^{-1}), without liquid trickling, there was no significant change in the TCE EC, which indicates that diffusion in the biofilm or biological kinetics became limiting. The maximum observed TCE EC without trickling liquid was 2.09 g m_{bed}^{-3} h^{-1}. Examination of analytical solutions for gaseous concentrations for zero-kinetics with either diffusion limitation or reaction limitation developed by Ottengraf and Van Den Oever [35,36] reveals that a reaction limitation was the most plausible explanation and is consistent with the constant EC obtained at various TCE concentrations (Fig. S3).

5. Conclusions

In this study, the rate-limiting step of an anaerobic biotrickling filter removing TCE vapors was analyzed after significant biomass build-up occurred. The TCE ECs at all conditions were up to 60% lower than prior to the important biomass build-up and warranted further investigations. A complex behavior was observed. At high liquid velocities, the biotrickling filter, which was operated with gas and liquid flowing co-currently, experienced bubbling, thus resulting in gas–liquid mass transfer limitation. At the lowest liquid velocity, gas–liquid mass transfer was limited at the liquid film, while at an intermediate liquid velocity gas–liquid mass transfer was limited at the gas film. A likely reason for the gas–liquid mass transfer limitations was the decrease in specific surface area, as a result of biomass growth on the spherical packing. The TCE ECs at any gas velocity without trickling liquid and in absence of biological limitation were higher than with trickling liquid, consistent with the observation that gas–liquid mass transfer was rate-limiting. Nonetheless, at the highest gas velocity tested without trickling liquid, the performance of the biotrickling filter was limited by biofilm phenomena. Overall, these investigations highlight mass transfer and kinetic limitations that can occur in biotrickling filters for air/gas pollution control and how they are dependent on the operating conditions.

Appendix A. Nomenclature

a_w	specific (wetted) interfacial area
C_G	gas concentration (subscripts: in = inlet, out = outlet)
C_L	liquid concentration (subscript: out = outlet)
H	Henry's constant
V_b	biotrickling filter bed volume
Q_L	liquid flow rate
Q_G	gas flow rate
$k_L a_W$	liquid film mass transfer coefficient × interfacial area
$k_G a_W$	gas film mass transfer coefficient × interfacial area
$K_L a_W$	overall mass transfer coefficient × interfacial area
$K_G a_W$	overall mass transfer coefficient × interfacial area
n	number of individual packing spheres in contact

Greek letter

ε	biotrickling filter bed porosity
η_0	global effectiveness factor

Appendix B. Supplementary data

Supplementary data associated with this article can be found, in the online version, at doi:10.1016/j.procbio.2009.11.017.

References

[1] Devinny JS, Deshusses MA, Webster TS. Biofiltration for air pollution control. Boca Raton, FL: CRC-Lewis Publishers; 1999.
[2] Kennes C, Veiga MC. Conventional biofilters. In: Kennes C, Veiga MC, editors. Bioreactors for waste gas treatment. Dordrecht, The Netherlands: Kluwer Academic Publishers; 2001. p. 47–98.
[3] Cox HHJ, Deshusses MA. Biotrickling filters. In: Kennes C, Veiga MC, editors. Bioreactors for waste gas treatment. Dordrecht, The Netherlands: Kluwer Academic Publishers; 2001. p. 99–131.
[4] Gabriel D, Deshusses MA. Retrofitting existing chemical scrubbers to biotrickling filters for H_2S emission control. Proc Natl Acad Sci USA 2003;100:6308–12.
[5] Prado OJ, Redondo RM, Lafuente J, Gabriel D. Retrofitting of an industrial chemical scrubber into a biotrickling filter: performance at a gas contact time below 1s. J Environ Eng ASCE 2009;135:359–66.
[6] Cox HHJ, Deshusses MA. Biological waste air treatment in biotrickling filters. Curr Opin Biotechnol 1998;9:256–62.
[7] Cox HHJ, Nguyen TT, Deshusses MA. Toluene degradation in the recycle liquid of biotrickling filters for air pollution control. Appl Microbiol Biotechnol 2000;54:133–7.
[8] Koe LLC, Yang F. A bioscrubber for hydrogen sulphide removal. Water Sci Technol 2000;41:141–5.
[9] Smet E, Lens P, Van Langenhove H. Treatment of waste gases contaminated with odorous sulfur compounds. Crit Rev Environ Sci Technol 1998;28:89–117.
[10] Shinabe K, Oketani S, Ochi T, Kanchanatewee S, Matsumura M. Characteristics of hydrogen sulfide removal in carrier-packed biological deodorization system. Biochem Eng J 2000;5:209–17.
[11] Kim S, Deshusses MA. Understanding the limits of H_2S degrading biotrickling filters using a differential biotrickling filter. Chem Eng J 2005;113:119–26.
[12] Gabriel D, Deshusses MA. Performance of a full-scale biotrickling filter treating H_2S at a gas contact time of 1.6 to 2.2 s. Environ Prog 2003;22:111–8.
[13] Goncalves JJ, Govind R. Enhanced biofiltration using cell attachment promotors. Environ Sci Technol 2009;43:1049–54.
[14] Lobo R, Revah S, Viveros-Garcia T. An analysis of a trickle-bed bioreactor: carbon disulfide removal. Biotechnol Bioeng 1999;63:98–109.
[15] Volpe A, Del Moro G, Rossetti S, Tandoi V, Lopez A. Remediation of PCE-contaminated groundwater from an industrial site in southern Italy: a laboratory-scale study. Process Biochem 2007;42:1498–505.
[16] Popat SC, Deshusses MA. Reductive dehalogenation of trichloroethene vapors in an anaerobic biotrickling filter. Environ Sci Technol 2009;43:7856–61.
[17] Rittmann BE, McCarty PL. Environmental biotechnology: principles and applications. New York, NY: McGraw-Hill Publishing Co.; 2001.
[18] Ottengraf SPP. Exhaust gas purification. In: Rhen H, Reed G, editors. Biotechnology. Weinheim, Germany: VCH Verlagsgesellschaft; 1986.
[19] Guthrie JP. Hydration of carboxylic acids and esters. evaluation of the free energy change for addition of water to acetic and formic acids and their methyl esters. J Am Chem Soc 1973;95:6999–7003.
[20] Hine J, Mookerjee PK. Structural effects on rates and equilibriums. XIX. The intrinsic hydrophilic character of organic compounds. Correlations in terms of structural contributions. J Org Chem 1975;40:292–8.
[21] Gossett JM. Measurement of Henry's law constants for C1 and C2 chlorinated hydrocarbons. Environ Sci Technol 1987;21:202–8.
[22] Fortin NY, Deshusses MA. Treatment of methyl *tert*-butyl ether vapors in biotrickling filters. 2. Analysis of the rate-limiting step and behavior under transient conditions. Environ Sci Technol 1999;33:2987–91.
[23] Cox HHJ, Sexton T, Shareefdeen ZM, Deshusses MA. Thermophilic biotrickling filtration of ethanol vapors. Environ Sci Technol 2001;35:2612–9.
[24] Aulenta F, Beccari M, Majone M, Petrangeli Papini M, Tandoi V. Competition for H_2 between sulfate reduction and dechlorination in butyrate-fed anaerobic cultures. Process Biochem 2008;43:161–8.
[25] Whitman WG. The two-film theory of gas absorption. Chem Met Eng 1923;29:146–50.
[26] de Santos JM, Melli TR, Scriven LE. Mechanics of gas–liquid flow in packed-bed contactors. Annu Rev Fluid Mech 1991;23:233–60.
[27] Doan HD, Wu J, Jedari Eyvazi M. Effect of liquid distribution on the organic removal in a trickle bed filter. Chem Eng J 2008;139:495–502.
[28] Kim S, Deshusses MA. Determination of mass transfer coefficients for packing materials used in biofilters and biotrickling filters for air pollution control. 1. Experimental results. Chem Eng Sci 2008;63:841–55.
[29] Satterfield CN. Trickle-bed reactors. AIChE J 1975;21:209–28.
[30] Devinny JS, Ramesh J. A phenomenological review of biofilter models. Chem Eng J 2005;113:187–96.
[31] Alonso C, Suidan MT, Sorial GA, Lee Smith F, Biswas P, Smith PJ, et al. Gas treatment in trickle-bed biofilters: biomass, how much is enough? Biotechnol Bioeng 1997;54:583–94.
[32] Dullien FAL. Porous media. Fluid transport and pore structure. New York, NY: Academic Press; 1979.
[33] Wolff F. Biologische Abluftreinigung mit einem intermittierend befeuchteten Tropfkörper. In: Dragt AJ, Van Ham J, editors. Biotechniques for air pollution abatement and odour control policies. Amsterdam, The Netherlands: Elsevier Science Publishers; 1992. p. 49–62.
[34] Pol A, Van Haren FJJ, Op den Camp HJM, Van der Drift C. Styrene removal from waste gas with a bacterial biotrickling filter. Biotechnol Lett 1998;20:207–10.
[35] Ottengraf SPP, Van Den Oever AHC. Kinetics of organic compound removal from waste gases with a biological filter. Biotechnol Bioeng 1983;25:3089–102.
[36] Ottengraf SPP. Exhaust gas purification. In: Schoenborn W, editor. Biotechnology: a comprehensive treatise, vol. 8. Microbial degradations. New York, NY: VCH Publishers, Inc.; 1986. p. 425–52.

Supporting Information for

Analysis of the Rate-limiting Step of an Anaerobic Biotrickling Filter Removing TCE Vapors

Sudeep C. Popat, Marc A. Deshusses

Pages: 10 (including cover page)

Figures: 4

Tables: 4

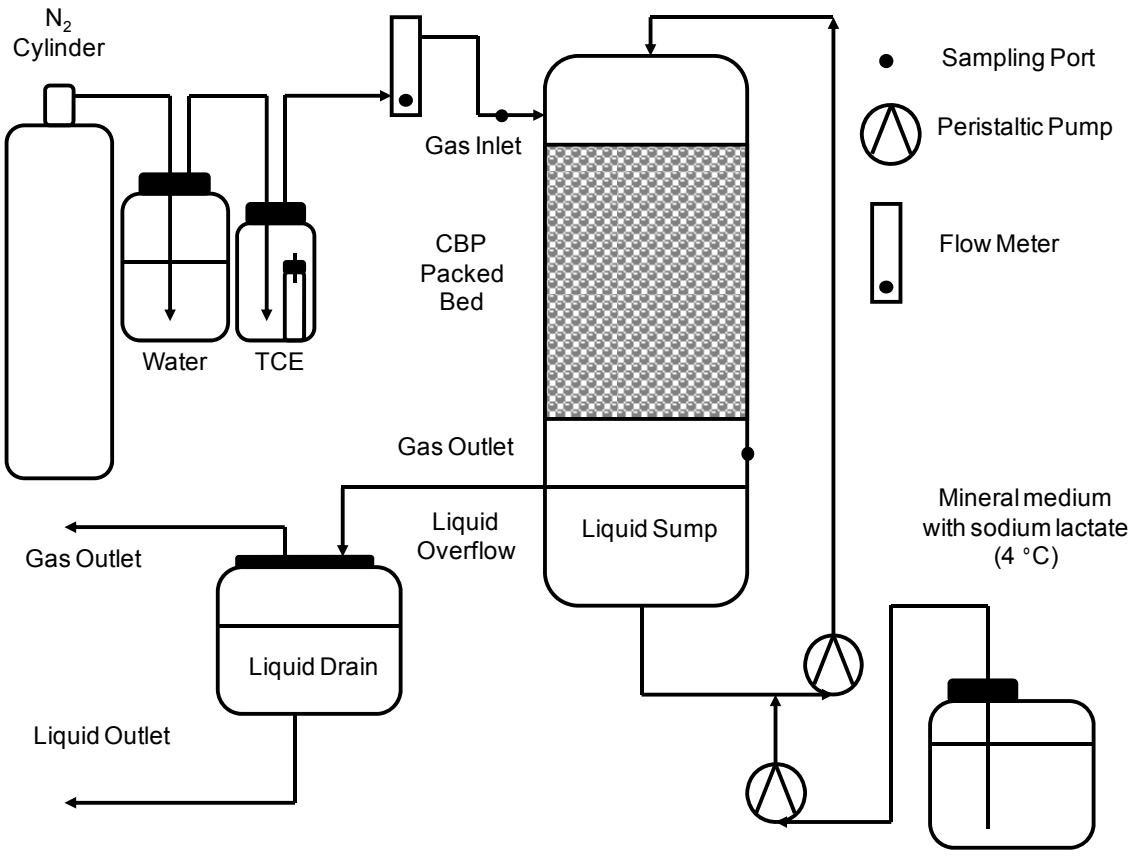

Figure S1. Schematic of the anaerobic biotrickling filter removing TCE.

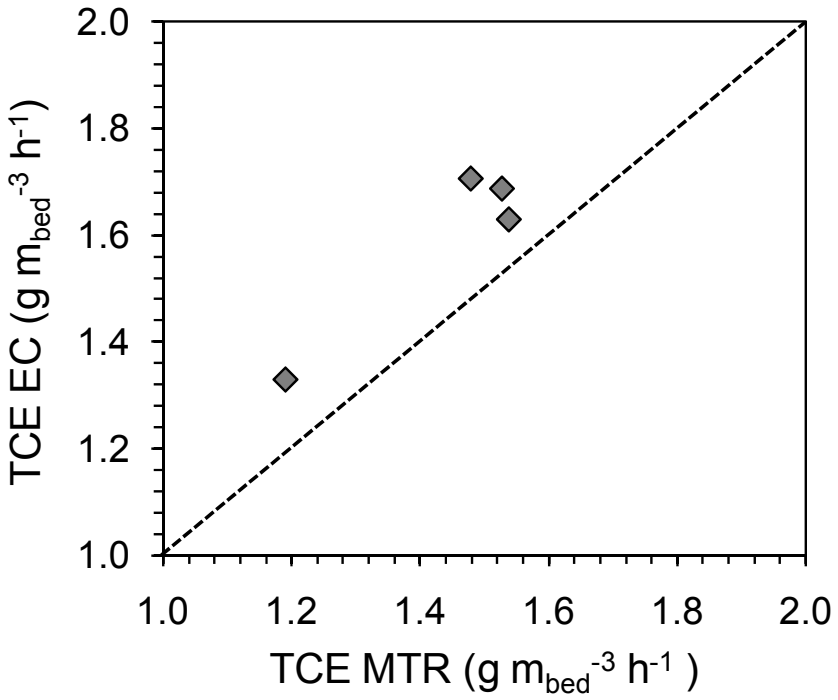

Figure S2. Comparison of TCE elimination capacity observed experimentally and the maximum TCE mass transfer rate (MTR) as calculated from the overall mass transfer coefficient ($K_L = \left(\frac{1}{k_L} + \frac{1}{H \cdot k_G} \right)^{-1}$) and overall liquid driving force. Experimentally determined gas and liquid concentrations were used for the calculation of MTR. The concentration in the liquid was assumed to be constant, while inlet and outlet concentrations were used for the gas; a log mean was taken for the average driving force. The diagonal line shows y=x.

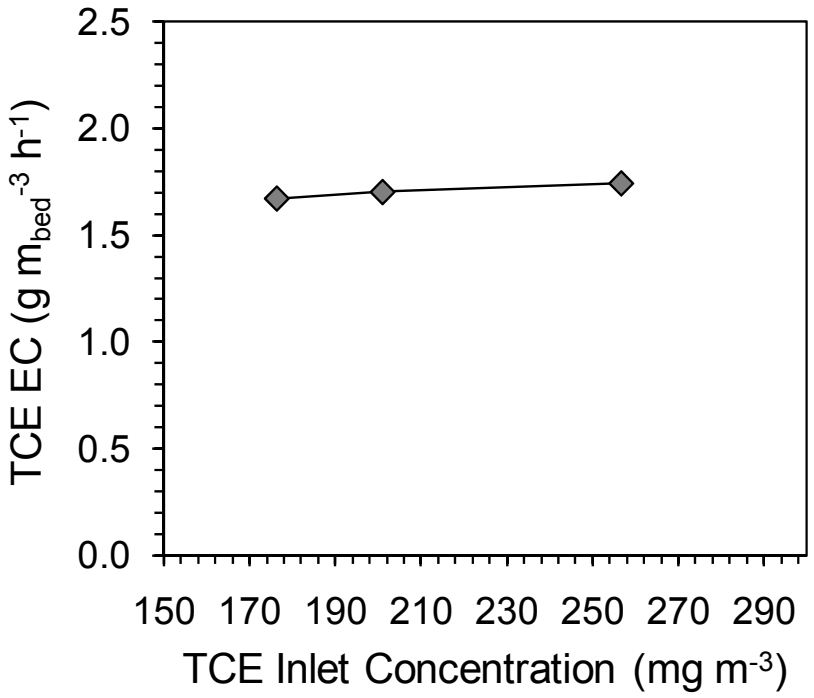

Figure S3. Effect of TCE inlet concentration on TCE elimination capacity at a gas velocity of 4.59 m h^{-1}.

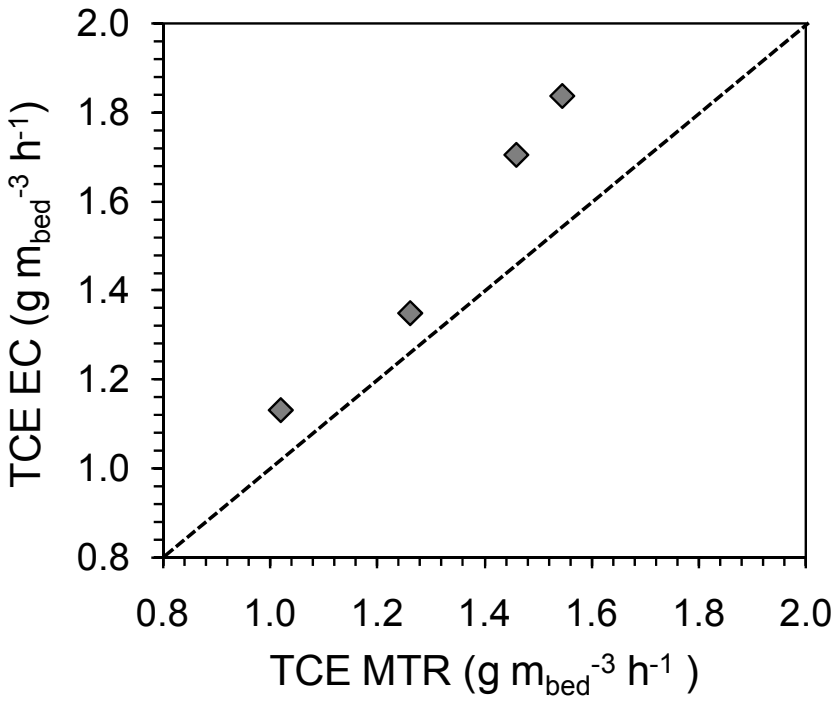

Figure S4. Comparison of TCE elimination capacity observed experimentally and the maximum TCE mass transfer rate (MTR) as calculated from the overall mass transfer coefficient ($K_G = \left(\frac{1}{k_G} + \frac{H}{k_L} \right)^{-1}$) and overall gas driving force. Experimentally determined gas and liquid concentrations were used for the calculation of MTR. The concentration in the liquid was assumed to be constant, while inlet and outlet concentrations were used for the gas; a log mean was taken for the average driving force. The diagonal line shows y=x.

Table S1. Definition of global effectiveness factor.

Global Effectiveness Factor

$$\eta_0 = \frac{\frac{1}{k\eta_S a_S}}{\frac{1}{k\eta_S a_S} + \frac{1}{k_L \eta_L a_W}}$$

where,

η_0 = global effectiveness factor

$\frac{1}{k\eta_S a_S}$ = resistance to overall removal from biofilm phenomena

$\frac{1}{k_L \eta_L a_W}$ = resistance to overall removal from gas-liquid mass transfer

k = superficial kinetic constant for biofilm phenomena

k_L = liquid film mass transfer coefficient

a_S = liquid-biofilm specific interfacial area

a_W = gas-liquid specific interfacial area

η_S = biofilm phenomena effectiveness factor

η_L = gas-liquid mass effectiveness factor

Note that this definition of the global effectiveness factor is derived assuming liquid film resistance to be governing gas-liquid mass transfer. If gas film resistance governs gas-liquid mass transfer, all liquid film terms will change to gas film terms.

Thus, if $\frac{1}{k\eta_S a_S} = \frac{1}{k_L \eta_L a_W}$ (i.e. equal resistance from biofilm phenomena and gas-liquid mass transfer), $\eta_0 = 0.5$. For $\eta_0 < 0.5$, $\frac{1}{k_L \eta_L a_W} > \frac{1}{k\eta_s a_S}$ and thus removal is limited by gas-liquid mass transfer, and for $\eta_0 > 0.5$, $\frac{1}{k\eta_S a_S} > \frac{1}{k_L \eta_L a_W}$ and thus removal is limited by biofilm phenomena.

Biofilm Phenomena Effectiveness Factor

$$\eta_S = \frac{1}{1 + \frac{k_B \eta}{k_S a_B}} = \frac{1}{1 + \frac{k}{k_S}} = \frac{\frac{1}{k}}{\frac{1}{k} + \frac{1}{k_S}}$$

where,

η = catalytic biofilm effectiveness factor

k_B = biodegradation rate constant

k_S = liquid-biofilm mass transfer coeffcient

a_B = biofilm specific external surface area

Gas-liquid Effectiveness Factor

$$\eta_L = \frac{1}{1+\frac{k_L}{Hk_G}} = \frac{\frac{1}{k_L}}{\frac{1}{k_L}+\frac{1}{Hk_G}}$$

where,

k_G = gas film mass transfer coefficient

Derivation of Eq. (2)

Assuming quasi-steady state,

$$N_{GL}\frac{dA_{GL,i}}{dV_L} = N_B\frac{dA_{LB,i}}{dV_L}$$

where,

N_{GL} = substrate flux from gas to liquid

N_B = substrate flux from liquid to biofilm

A_{GL} = gas-liquid interfacial area

A_{LB} = liquid-biofilm interfacial area

V_L = liquid volume

Thus using definition of individual fluxes,

$$k_L\eta_L a_W\left(\frac{C_G}{H}-C_L\right) = k\eta_s a_s C_L$$

Substituting in the definition of global effectiveness factor,

$$\eta_0 = \frac{\frac{1}{k\eta_S a_S}}{\frac{1}{k\eta_S a_S}+\frac{1}{k_L\eta_L a_W}} = \frac{\frac{C_L}{k_L\eta_L a_W\left(\frac{C_G}{H}-C_L\right)}}{\frac{C_L}{k_L\eta_L a_W\left(\frac{C_G}{H}-C_L\right)}+\frac{1}{k_L\eta_L a_W}} = \frac{C_L}{C_L+\left(\frac{C_G}{H}-C_L\right)} = \frac{H\cdot C_L}{C_G}$$

Table S2. Composition of modified RAM media.

Compound	**Concentration (g L^{-1})**
KH_2PO_4	0.27
K_2HPO_4	0.35
NH_4Cl	0.53
$CaCl_2 \cdot 2H_2O$	0.075
$MgCl \cdot 6H_2O$	0.1
$FeCl_2 \cdot 4H_2O$	0.02
$NaHCO_3$	0.2
Trace elements	5 (mL L^{-1})
Yeast extract	1.0

Table S3. Effect of liquid velocity on $\eta_{0,TCE}$, $\eta_{0,cis\text{-}DCE}$, $\eta_{0,VC}$ and $\eta_{0,ETH}$ at a as velocity of 4.59 m h^{-1}.

Liquid velocity (m h^{-1})	**$\eta_{0,TCE}$ (-)**	**$\eta_{0,cis\text{-}DCE}$ (-)**	**$\eta_{0,VC}$ (-)**	**$\eta_{0,ETH}$ (-)**
0.08	0.13	1.51	3.13	11.23
0.27	0.34	1.07	2.35	10.16
0.36	0.30	1.11	2.07	9.79
0.59	0.36	0.98	1.81	9.76

Table S4. Effect of gas velocity on $\eta_{0,TCE}$, $\eta_{0,cis\text{-}DCE}$, $\eta_{0,VC}$ and $\eta_{0,ETH}$ at a liquid velocity of 0.27 m h^{-1}.

Gas velocity (m h^{-1})	**$\eta_{0,TCE}$ (-)**	**$\eta_{0,cis\text{-}DCE}$ (-)**	**$\eta_{0,VC}$ (-)**	**$\eta_{0,ETH}$ (-)**
2.68	0.23	1.29	2.53	12.76
3.82	0.29	1.08	2.39	10.24
4.59	0.34	1.11	2.35	9.79
6.11	0.44	0.98	1.81	4.74